J. Membrane Biol. 115, 261–272 (1990)

The Journal of
Membrane Biology

Water Transport and Estimated Transmembrane Potential during Freezing of Mouse Oocytes

M. Toner†, E.G. Cravalho†, and D.R. Armant‡*

†Harvard University-Massachusetts Institute of Technology, Division of Health Sciences and Technology, and Massachusetts Institute of Technology, Department of Mechanical Engineering, Cambridge, Massachusetts, and ‡Charles Dana Biomedical Research Institute, Beth Israel Hospital and Harvard Medical School, Boston, Massachusetts

Summary. The kinetics of water transport and the changes in transmembrane potential during freezing of mouse oocytes in isotonic phosphate buffered saline (PBS) were simulated using thermodynamic models. The permeability to water at 0°C, L_{pg}, and the activation energy, E_{Lp}, of metaphase II mouse oocytes from $B_6D_2F_1$ mice were determined to be 0.044 ± 0.008 μm/min-atm and 13.3 ± 2.5 kcal/mol during freezing at 2°C/min. The inactive cell volume was determined to be 0.214 with a correlation coefficient of 0.995, indicating that the oocytes closely follow the ideal Boyle-van't Hoff relation. The mean value of the oocyte diameter was 79.41 ± 4.62 μm. These results were used to predict the behavior of mouse oocytes under various freezing conditions. The effect of the cooling rate on the cell volume and cytoplasm undercooling was investigated.

The changes in transmembrane potential were also investigated during freezing of mouse oocytes. The computer simulations showed that at the beginning of the freezing process (−1°C), the fast growth of ice in the extracellular solution causes a sharp increase of the membrane potential. It is predicted that the change in membrane potential is substantial for almost all cooling rates. Estimations show that values as high as −90 mV may be reached during freezing. The hyperpolarization of the membrane may cause orientation of the dipoles within the membrane. For membrane proteins with 300 debye dipole moment, the theoretical prediction suggests that the percentage of dipoles aligned with the membrane potential increases from 16% at 0°C prior to freezing to 58% at −8°C after seeding of the external ice followed with a cooling at 120°C/min.

Key Words water transport · ion transport · permeability · oocytes · freezing

Introduction

The mass transport of water across the plasma membrane and the amount of water remaining within the cell during freezing play a very significant role in cell damage. In recent years, several models have been developed to describe the physicochemical events occurring during the freezing and thawing of biological cells. The first of such models was due to Mazur in 1963. Mazur developed a mathematical model to predict the water content of cells subjected to freezing, the essence of which became the basis of almost all subsequent treatments (Mansoori, 1975; Silvares et al., 1975; Scheiwe & Koerber, 1983). Briefly, for a cell suspended in a freezing medium and subjected to sub-freezing temperatures, ice preferentially forms outside the cell in the freezing medium. Due to the precipitation of the pure ice, the water in the partially frozen extracellular solution has a lower chemical potential than the water in the intracellular solution. As a result, the thermodynamic equilibrium that exists across the cell membrane between the cell contents and the freezing medium is upset, and the cell responds by expressing water across the cell membrane. Three biophysical parameters that are shown to be important in determining the thermodynamic states of intracellular solution during freezing are: (i) surface area-to-volume ratio (SA/V); (ii) the hydraulic conductivity of the plasma membrane (L_{pg}); and (iii) the activation energy of the hydraulic conductivity (E_{Lp}, i.e., its temperature dependence). Mazur's model predicts that high SA/V and L_{pg}, and low E_{Lp} values would increase the water transport during a freezing protocol. It is imperative to determine these three biophysical parameters to understand the freeze/thaw response of cells.

The sole effect of external ice formation during freezing of biological cells is not the water efflux. One also needs to investigate the diffusion of ionic species during freezing. It is well known from electro-diffusion theories that any alteration in the ionic composition of the suspending medium will result in a nonsteady-state movement of ions across the

Current address: Wayne State University, Medical School, Department of Obstetrics and Gynecology, Detroit, MI.

plasma membrane. The bulk of the cytoplasm and the external solution is electrically neutral with an equal number of positive and negative charges. However, cells have an electrical charge layer on their plasma membrane resulting from a charge separation over a very narrow region on either side of the membrane (Kotyk, Janacek & Koryta 1988). This separation of charge is responsible for the resting membrane potential, E_R. The more general term *membrane potential* (E_m) refers to the potential across the membrane at any moment, including resting and activation states of the membrane. Thus, any change in the ionic strength of the intra- and/or extra-cellular solutions will alter the transmembrane potential as well. Although the Goldman-Hodgkin-Katz (GHK) theory has been widely used to investigate the membrane potential of many biological cells (Goldman, 1943; Hodgkin & Katz, 1949), there have been cases where the model did not adequately describe the electrochemical phenomena (Ohki, 1986; Pethig, 1986). Given the uncertainties involved in experimental techniques and the theoretical difficulties associated with a very complex situation such as freezing of cells, we have decided to use GHK theory in our analysis. This will give us an order-of-magnitude estimate of the changes occurring in the plasma membrane during freezing.

Leibo (1980) and Jackowiski, Leibo and Mazur (1980) have measured the water permeability and cryoprotectant permeabilities of unfertilized and fertilized mouse ova at suprazero temperatures. Leibo, McGrath and Cravalho (1978) also determined the ice-nucleation temperature of mouse oocytes in the presence of 1 M dimethylsulfoxide (Me_2SO) and Rall, Mazur and McGrath (1983) have determined the intracellular ice formation temperatures of 8-cell mouse embryos. Mazur (1984) used this information to predict the freezing behavior of mouse ova showing qualitative agreement between theory and experiment opening the way for further quantitative studies. Recently, Bernard et al. (1988) determined the water permeability of mouse oocytes at 21°C using a diffusion chamber. None of these studies have determined the water permeability of mouse oocytes at subzero temperatures in the presence of extracellular ice. In addition to water transport, the only time that the theory of electrodiffusion was applied to freezing of cells was Silvares's (1974) work on red blood cells. Silvares showed that the application of GHK theory for freezing can adequately describe the changes in membrane potential. It is the purpose of this study to quantify both water transport across the plasma membrane and the changes in transmembrane potential of mouse oocytes without cryoadditives to better understand the physicochemical events occurring during freezing.

Theoretical Background

Kinetics of Water Transport

To model the flow of water across a biological membrane, the following equation can be written from entropy generation arguments, assuming that equilibria of temperature and pressure prevail between the intra- and extracellular media (Mazur, 1963).

$$\frac{dV}{dt} = -\frac{L_p RT}{v_w} A \left(\ln a_w^{ex} - \ln a_w^{in}\right) \tag{1}$$

where V, cell volume; t, time; L_p, water permeability; R, gas constant; T, absolute temperature; A, surface area of the cell; v_w, partial molar volume of water; and a_w^{ex} and a_w^{in} water activities in the extra- and intracellular solutions, respectively.

During freezing, a cell is subjected to an environment that is continuously changing in osmolality as pure water freezes out of the extracellular medium. A Gibbs-Helmholtz relation can be used to relate extracellular concentration to temperature at constant pressure (Modell & Reid, 1983)

$$\frac{d}{dT}(\ln a_w^{ex})_P = \Delta H_f / RT^2 \tag{2}$$

where ΔH_f is the heat of fusion of water. If ΔH_f is considered constant, Eq. (2) can be integrated yielding

$$\ln a_w^{ex} = \frac{\Delta H_f}{R}\left(\frac{1}{T_R} - \frac{1}{T}\right) \tag{3}$$

where T_R is the equilibrium freezing temperature of pure water (273.15 K). Other studies have assumed that ΔH_f varied with temperature (Mazur, 1963; Schwartz & Diller, 1983*a*), but it was found in this study that the effect of this variation was not significant.

The intracellular solution is modelled as an ideal solution for which the water activity is equal to its mole fraction

$$x_w^{in} = \frac{n_w}{n_w + (v_s n_s)} = \frac{(V - V_b)}{(V - V_b) + v_w(v_s n_s)} \tag{4}$$

where n_w and n_s, number of moles of water and solutes in the cell; v_s (= 2), the dissociation con-

stant; and V_b, inactive cell volume. It is assumed that permeability is rate-limited by the passage of water through the cell membrane. Therefore, the temperature dependence can be expressed as an Arrhenius relationship (Levin, Cravalho & Huggins, 1976)

$$L_p = L_{pg} \exp\left[-\frac{E_{Lp}}{R}\left(\frac{1}{T} - \frac{1}{T_R}\right)\right] \tag{5}$$

where L_{pg} is the permeability to water of the cell membrane at T_R and E_{Lp} is the apparent activation energy for the permeation process. In this study, the permeability reference temperature, T_R, was chosen to be the freezing point of pure water (273.15K) instead of room temperature (293.15K) as is more traditionally used (Leibo, 1980; Schwartz & Diller, 1983*a*). The reason for this choice is that this study concerns osmotic behavior in the subzero temperature range.

If temperature is changed linearly with time, a transformation from temperature to time can be made by introducing a cooling rate B

$$B = -\frac{dT}{dt}. \tag{6}$$

Substituting Eqs. (3) and (4) into Eq. (1) and using Eq. (6) to transform from time to temperature yields an expression for rate of cell volume change during freezing

$$\frac{dV}{dT} = \frac{L_p A R T}{v_w B}\left[\ln\left(\frac{V - V_b}{V - V_b + v_w(v_s n_s)}\right) - \frac{\Delta H_f}{R}\left(\frac{1}{T_R} - \frac{1}{T}\right)\right] \tag{7}$$

where L_p is specified in Eq. (5) and A is specified as follows:

$$A = A_o(V/V_o)^{2/3} \tag{8}$$

where A_o and V_o are the initial surface area and volume of the oocytes, respectively. The effect of the constant cell surface area rather than a 2/3rds power dependence of A upon V has negligible (<10%) effect upon the resulting permeability parameters (Levin, Ushiyama & Cravalho, 1979; Callow & McGrath, 1985). Thus, a theoretical temperature-volume history of a cell during freezing can be predicted by integrating Eqs. (7) and (8) subject to the initial condition $V = V_o$ at seeding temperature, i.e., extracellular ice formation temperature, of the extracellular medium.

Transmembrane Potential

The equations used almost exclusively at present for describing passive transport of ions and membrane potential across the plasma membranes are derived by Goldman (1943) and called constant-field equations. Generally, only the most common ions, K^+, Na^+, and Cl^- are taken into account. Hodgkin and Katz (1949) made use of partition (or distribution) coefficients to relate the ionic concentrations at the inner and outer surface of the plasma membrane to the bulk ionic concentrations. This modified constant-field equation describing the membrane potential is known as the Goldman-Hodgkin-Katz (GHK) equation. According to GHK, the membrane potential of a cell, E_m, is determined by the concentrations of exchangeable K^+, Na^+, and Cl^- in the cell and the membrane permeabilities of these ions and can be estimated as follows:

$$E_m = \frac{RT}{F} \ln \frac{P_K[K^+]^{ex} + P_{Na}[Na^+]^{ex} + P_{Cl}[Cl^-]^{in}}{P_K[K^+]^{in} + P_{Na}[Na^+]^{in} + P_{Cl}[Cl^-]^{ex}} \tag{9}$$

where F is the Faraday constant. The GHK equation in the above form neglects the possible complications caused by the effects of electrogenic pumps on the membrane potential. The use of the GHK equation in the presence of an electrogenic pump in the frog muscle was analyzed by Geduldig (1968). His result suggests that if pumps are only "slightly" electrogenic (i.e., less than 10^{-11} mol/cm^2/sec) the net diffusion current will not substantially affect the constant field equation. Since the active fluxes of Na^+ and K^+ were found to be 24×10^{-12} and 9×10^{-12} mol/cm^2/sec for mouse oocytes (Powers & Tupper, 1975), the constant field equation will be assumed to retain its validity. In addition, Frumento (1965) included the effect of active transport in the constant field equation. However, the active transport can be neglected at subzero temperatures (Frumento, 1965; Biggers, Borland & Powers, 1977). Equation (9), in its present form, neglects the effect of the membrane potential independent Na-K-2Cl exchanger (Geck & Heinz, 1986).

Materials and Methods

Cryomicroscopy and Image Analysis

The apparatus used to cool and observe the oocytes consisted of a Zeiss Universal light microscope, a video camera (Ikegami ITC 62), a color monitor (Panasonic S1300), a video cassette recorder (Panasonic 6300), a specially designed cryostage, a system consisting of a computer-based temperature controller and a video-interface, and published in detail elsewhere (Cosman et al.,

1989). The temperature controller is based on the design of Diller and Cravalho (1970), and the video-interface is based on the work of Cosman (1983). A *sapphire* plate (Adolf Meller Co., Providence, RI) of 1.6 mm was employed on the heating window to reduce the temperature gradients as described elsewhere (Cosman et al., 1989). The temperature difference across the heating window (10 mm) was *less* than 0.1°C. This eliminated experimental errors in the determination of the permeability parameters.

Following each experiment, the videotape was reviewed in order to measure the volume variation of each oocyte. To make these measurements, individual frames were converted from videotape to digital format using a Digi-View hardware/software system (NewTek, Topeka, KS) and an Amiga 1000 computer (Commodore, West Chester, PA). The frames were digitized in a 320 × 200 spatial format in x-y coordinates with 4 bits (16 discrete values) of gray-level resolution. After the frames were digitized, they were stored as IFF files on 3.5 inch, 880K diskettes (Orrico, 1988).

Experimental volume/temperature curves were generated from these digitized images. The projected cross-sectional area was measured by tracing the cell boundary using a mouse controlled cursor. A program electronically counted the number of pixels in the enclosed area. By assuming spherical symmetry, the projected area was converted to volume using the following relation:

$$V = (PA)^{3/2}/(6\sqrt{\pi}) \tag{10}$$

where PA is the projected area. A number of calibration studies were performed to test the accuracy of the technique and to find the conversion factor for the number of pixels to square microns. In these experiments microspheres of approximately 90 μm (Polyscience 7315, Warrington, PA) were placed on a slide etched with a calibrated scale (1/100 mm, Zeiss), and their diameter was measured optically under the microscope. The microspheres were also recorded on video tape and their images digitized. The variability in the three measurements was less than 2% for each sphere (Orrico, 1988).

Collection, in-Vitro Fertilization of Mouse Oocytes and Culture of Embryos

The procedures for the collection and fertilization of mouse oocytes were essentially those described previously (Jackson & Keissling, 1989; Toner, Cravalho & Armant, 1990*a*). Briefly, oocytes and sperm were collected from $B_6D_2F_1$ mice (4 to 6 weeks old) available from Jackson Laboratory (Bar Harbor, ME). Female mice were induced to superovulate by means of intraperitoneal injection of 5 IU of pregnant mare serum gonadotrophin (PMSG, Sigma, St. Louis, MO) followed 48 hours later by injection of human chorionic gonadotrophin (hCG, Sigma). Twelve to 15 hours later metaphase II oocytes were collected and used for control experiments. The medium for fertilization *in-vitro* and subsequent development was a slight modification of Earle's balanced salt solution (EBSS, powder, Sigma) as described in Jackson and Keissling (1989).

Static Experiments and Diameter Measurement

Static (or equilibrium) experiments were necessary to determine the osmotically inactive volume, V_b, of oocytes to solve Eq. (7). Oocytes was allowed to equilibrate in hypertonic solutions having osmolalities ranging from 557 to 2,215 mosm/kg at ambient temperature. The hypertonic solutions were made by adding NaCl to Dulbecco's phosphate buffered saline (PBS). Each solutions' osmolality was calculated (Weast, 1973) and checked by an osmometer (Advanced Instruments Model 3L).

Observations of the osmometric behavior of the oocytes were made on a Zeiss 405 ICM inverted microscope. Initially, each oocyte was placed in isotonic PBS and then transferred through drops of increasing hypertonicity covered with silicon oil to prevent evaporation. After the oocyte had equilibrated in the solution (in approximately 5 min), the dish was placed on the stage of the microscope, and the microscopic image of the oocyte was recorded on videotape for subsequent measurement. The volume of each oocyte was measured as described above, and the ratio of the equilibrium volume in hypertonic solution to the isotonic volume of each oocyte was found. The average volume ratio for each osmolality was calculated and plotted against the reciprocal of osmolality. The data points were then fitted by the method of least squares and the theoretical osmotically inactive volume was obtained by extrapolating the best fit line to an infinitely concentrated solution.

In addition to the osmometric behavior, the diameter distribution of oocytes was also determined using the same experimental procedure described above. Eighty oocytes were used for this purpose.

Subzero Permeability Experiments

In experiments conducted at subzero temperatures, culture dishes were removed from the incubator and mouse oocytes were transferred by pipette from Earle's medium to a culture dish containing PBS. The oocytes were then allowed to equilibrate in the PBS for about 10 min. A sample of 3 to 10 oocytes was then placed on the cryostage under a cover slip and sealed with silicon grease (Dow Corning, Midland, MI). The thickness of the sample was estimated to be between 150 to 300 μm. One to five of these oocytes were visible at one time in the field of view of the microscope. A 16× objective (Plan 16/0,35 Ph2, Zeiss) and a 2×-photo-ocular (Zeiss) were used. the extracellular medium was then seeded at approximately −1°C by touching the window of the cryostage with a small steel spatula cooled in liquid nitrogen. As soon as an ice front covered the field, the specimen was cooled at 2°C/min. The cooling and videotaping continued until a predetermined final temperature (−15 to −20°C) was reached. Experimental volume/temperature curves were obtained by measuring the volume of the oocyte approximately every 30 seconds (i.e., 1°C). The volume of the oocyte was measured as described above. No post-experimental viability test was run with the oocytes due to our inability to recover them from the freezing stage. Since the intracellular ice occurred at temperatures below -5°C under isothermal conditions (Toner et al. 1990*a*), the method of Schwartz and Diller (1983*b*) to determine the permeability of cells at constant subzero temperatures could not be adopted in this study.

Permeability Estimation Method

An iterative technique was used to obtain values for the permeability values that would produce the *best fit* between experimental volume measurements and theoretical volumes predicted by the model (Eq. (7)). This technique has already been employed several times in the estimation of permeability parameters (Stusnick & Hurst, 1972; Levin et al., 1979; Schwartz & Diller 1983*a*,*b*).

Briefly, the applied fitting technique minimized the difference between the theoretical (Eq. (7)) and experimental volume curves as judged by the value of the chi-squared statistics, χ^2. Two different methods were used to minimize χ^2. The gradient search method was employed for conditions far from convergence, and the linearization method was applied for conditions near convergence (*see* Levin et al., 1979, for a detailed discussion). Values of the transport coefficients, L_{pg} and E_{Lp}, were adjusted by iteration until the change in χ^2 between successive iterations converged to $\Delta\chi^2/\chi^2 < 0.01$.

Results

In-Vitro Fertilization and Subsequent Culture

The average fertilization rate for *control* experiments was 90% (715/796) and the percentage of fertilized ova that developed to blastocyst stage was 82% (583/715). The effects of using hyaluronidase to remove cumulus mass and cooling to 0°C (thermal shock) was also investigated (Toner et al., 1990*a*). No adverse effects were observed, and consequently oocytes were assumed to be viable at the beginning of the permeability experiments. No viability test could be run after the permeability experiments due to our inability to recover the oocytes from the freezing stage.

Osmometric Behavior

The results of the static experiments on mouse oocytes are indicated in Fig. 1. Regression of the data yields a linear relationship between equilibrium volume and the reciprocal of osmolality. The inactive volume fraction, V_b/V_o, for mouse oocytes at metaphase II was determined to be 0.213. The coefficient of correlation for the best-fit equation was 0.995. The value of the coefficient of correlation indicates that the oocytes closely follow the Boyle-van't Hoff relation.

The diameter measurements yielded a mean value diameter of 79.41 μm and a standard deviation of 4.62 μm. Figure 2 shows the experimental diameter distribution of metaphase II mouse oocytes.

Subzero Permeability Results

The permeability of 0°C, L_{pg}, and the activation energy, E_{Lp}, of mouse oocytes were determined simultaneously by fitting theoretically predicted volume/temperature curves (Eq. (7)) to experimentally measured volumes of oocytes between 0 and −16°C (Fig. 3) using nonlinear regression analysis as outlined above. The mean value and standard deviation

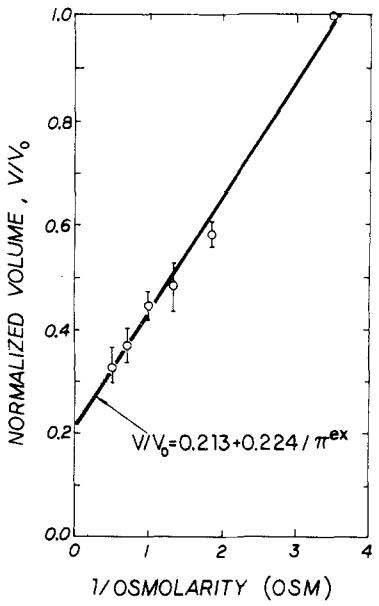

Fig. 1. Static osmometric behavior of mouse oocytes in different hypertonic saline solutions. Five oocytes were used for these experiments. Bars show the standard deviations

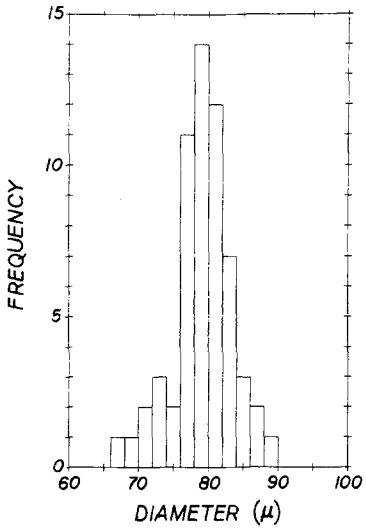

Fig. 2. Diameter distribution of mouse oocytes in isotonic saline solution. The mean diameter is 79.41 μm and the standard deviation is 4.62 μm

of L_{pg} were found to be 0.044 and 0.008 μm/min-atm for mouse oocytes. The mean value and standard deviation of E_{Lp} were found to be 13.3 and 2.5 kcal/mol, respectively. Since the assumption of spherical symmetry was made, only oocytes that shrunk in a reasonably spherical manner were used. For each of the eight experiments, χ^2 between the theoretical prediction of experiment was always less than 10^{-4}. The relatively small variation of the permeability parameters may be due to our very strin-

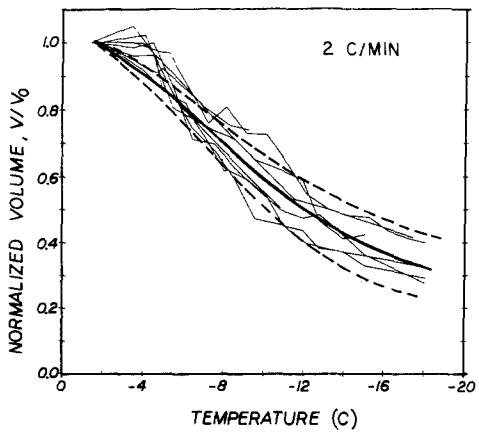

Fig. 3. Experimental measurement of normalized total volume at various temperatures for mouse oocytes cooled at 2°C/min. Eight oocytes are reported. Oocytes that deviated from the sphericity during dehydration were discarded to minimize the experimental errors. The temperature gradient over the whole field (10 × 10 mm) was less than 0.1°C. The solid line is the theoretical prediction using the mean values of permeability parameters (i.e., L_{pg} = 0.044 μm/min-atm and E_{Lp} = 13.3 kcal/mol). The top dashed line is the prediction using the upper limit of the permeability (i.e., L_{pg} + SD and E_{Lp} − SD), and the bottom dashed line is the prediction using the lower limit of the permeability (i.e., L_{pg} − SD and E_{Lp} + SD). SD is the standard deviation (*see* text)

gent experimental conditions such as: (i) only oocytes that remained spherical were used for data analysis; (ii) the temperature gradient across the window (10 × 10 mm) was reduced to less than 0.1°C by using the *sapphire* plate; and (iii) only metaphase II oocytes were used as suggested by the *control* experiments. The theoretical prediction solving Eq. (7) by 4th order Runge-Kutta scheme with a step size of 0.1°C is also depicted in Fig. 3.

Ion Transport Parameters

Estimates of internal ionic concentrations were determined by Powers and Tupper (1975). The exchangeable $[K^+]^{in}$, $[Na^+]^{in}$ and $[Cl^-]^{in}$ concentrations for mature oocyte are 204, 83, and 68 mM, respectively (Powers & Tupper, 1975). The concentration of the extracellular solution is equivalent to an isotonic PBS solution. Initially the system is assumed to be in electrochemical and osmotic equilibrium. The permeabilities of the plasma membrane to K^+, Na^+, and Cl^- are 8×10^{-8}, 12×10^{-8}, and 27×10^{-6} cm/sec, respectively (Powers & Tupper, 1975).

The external solution was assumed to be a saline (PBS) solution as NaCl was the major component. The external concentration was then estimated from the equilibrium phase diagram of NaCl between 0°C < T < −20°C (Weast, 1973) as follows:

$$[\text{NaCl}] = 0.0101\ T^3 - 4.31\ T^2 + 307.9\ T - 10.86 \quad (11)$$

where T is in Celsius and [NaCl] is in mM.

Discussion

Kinetics of Water Transport

The value of the fraction of the inactive oocyte volume (i.e., 0.213) correlated well with other studies. Leibo (1980) found essentially the same inactive cell volume of 0.18 for fertilized mouse ova. Abramczuk and Sawicki (1974) determined the concentration of dry mass of unfertilized and fertilized ova to be 18.3 and 19.0 g/100 cm^3, respectively. Assuming that the inactive cell components have the same density as proteins (1.33 g/cm^3), these dry mass measurements agree closely with the results of this study. Similar results were determined for 8-cell and blastocyst stage mouse embryos, 0.149 and 0.201, respectively (Mazur & Schneider, 1986). Bernard et al. (1988) determined that 20% of the volume of mouse oocytes was inactive. These results are also in agreement with the value of 21.6% for the inactive cell volume of hamster oocytes (Shabana & McGrath, 1988).

With respect to permeability parameters, Leibo (1980) reports a value of 0.44 μm/min-atm for permeability at 20°C and a value of approximately 14.5 kcal/mol for activation energy of mouse oocytes. If Leibo's value of L_p is extrapolated to 0°C using Eq. (5), one finds L_{pg} to be 0.071 μm/min-atm. This extrapolated value agrees closely with the L_{pg} for unfertilized ova found in this study. Figure 4 illustrates a comparison of permeabilities determined at subzero (this study) and suprazero (Leibo, 1980) temperatures as a function of temperature. For example, the extrapolation of permeability values from Leibo's suprazero temperature range measurements yield 0.026 and 0.015 μm/min-atm at −10 and −15°C, respectively. This correlates favorably with the values of 0.017 and 0.011 μm/min-atm at −10 and −15°C, respectively, determined in this study. The discrepancy may be explained by the differences in experimental conditions and/or the fact that the conductivity of water through biological membranes could be much lower than extrapolation of suprazero results would predict due to either membrane phase changes or decreased diffusion of water at subzero temperatures (Levin et al., 1976). In addition, Bernard et al. (1988) determined the water permeability of mouse oocytes at 21°C using a diffusion chamber. They report a value of 0.36 ± 0.07 μm/min-atm. If this value is extrapolated to

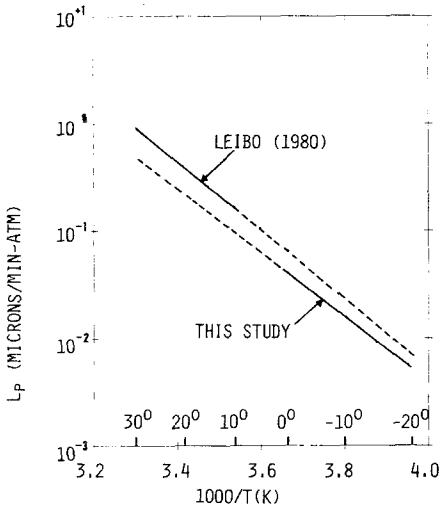

Fig. 4. Comparison of the water permeability values determined from subzero (this study) and suprazero (Leibo, 1980) temperatures. Between 0 and −20°C, L_{pg} = 0.044 μm/min-atm at 0°C and E_{Lp} = 13.3 kcal/mol. Between 30 and 10°C, L_{pg} = 0.44 μm/min-atm at 20°C and E_{Lp} = 14.5 kcal/mol

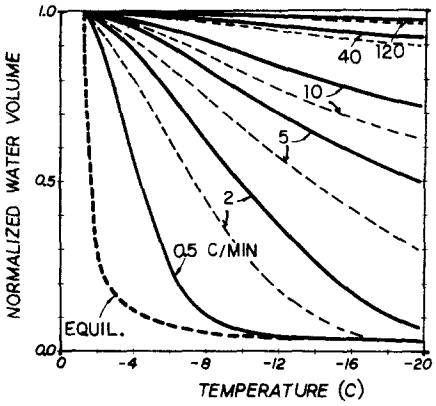

Fig. 5. Predicted temperature dependence of theoretical normalized water volume for mouse oocytes cooled at various rates. Extracellular seeding temperature is −0.615°C. The dashed curves are the theoretical prediction using the permeability measurements at suprazero temperatures by Leibo (1980)

0°C using an activation energy of 14.5 kcal/mol, one finds L_{pg} to be 0.053 μm/min-atm which agrees closely with the result of this study. In addition, Shabana and McGrath (1988) determined the water permeability of hamster oocytes to be 0.8 ± 0.1 μm/min-atm at 23°C using a diffusion chamber. However, they did not determine the value of the activation energy from their subzero experiments, instead they assumed a value of 14.5 kcal/mol based on the activation energy of mouse oocytes (Leibo, 1980).

The fact that the subzero temperature measurements from this study is in close agreement with the results of suprazero temperature measurements (Leibo, 1980), one would conclude that there does not seem to be a discontinuity of membrane water permeability between +30 and −20°C. This conclusion is in contrast with the result of Schwartz and Diller (1983*b*) with human granulocytes. Extrapolation of the nonfrozen permeability values to subzero temperatures indicated a lower permeability than the permeability determined at subzero temperatures for granulocytes. The differences is the behavior of mouse oocytes and human granulocytes may be explained by their sensitivity to the effects of the external ice formation on the cell membrane. For example, Tondorf, McGrath and Olien (1987) and Hendl, McGrath and Olien (1987) showed that cell-sized liposomes and mouse oocytes exhibit differences with respect to their adhesion to the external ice and subsequent shape deformation. However, more analysis is necessary to draw any quantitative conclusion.

Computer simulations of water transport from mouse oocytes during freezing were performed using the biophysical parameters determined in this study. Figure 5 shows the effect of the cooling rate, B, on the predicted displacement from equilibrium states for oocytes when the freezing starts at the equilibrium freezing point. The curve displays the normalized cell water volume as a function of temperature. The equilibrium curve represents the normalized water volume in a single oocyte cooled infinitely slowly to various subzero temperatures. This curve is generated from Eq. (7) assuming $dV/dT = 0$ at equilibrium. The figure illustrates a highly significant effect of the cooling rate on the water content of an oocyte at any subzero temperature. At −10°C the water content of the oocyte cooled at 2°C/min is 50% of its initial water content. At the same intermediate temperature the predicted water content of an oocyte cooled at a faster rate is higher. At rates about 40°C/min, the water transport is negligible. There is only 8 and 3% water loss from an oocyte cooled to −20°C at rates of 40 and 120°C/min, respectively. The predictions of computer simulations using the permeability parameters determined at suprazero temperatures (i.e., L_{pg} = 0.44 μm/min-atm at 20°C and E_{Lp} = 14.5 kcal/mol) are also illustrated in Fig. 5 for comparison purposes. As can be seen from this figure, the discrepancy between the volume curves estimated from subzero and suprazero permeability measurements become significant at slow cooling rates (<10°C/min). This suggests that the application of membrane permeability parameters obtained at suprazero temperatures is not acceptable for modelling the freezing process. Mazur (1984) also determined that the predicted volume fraction of a mouse ovum frozen in 1 M Me_2SO at

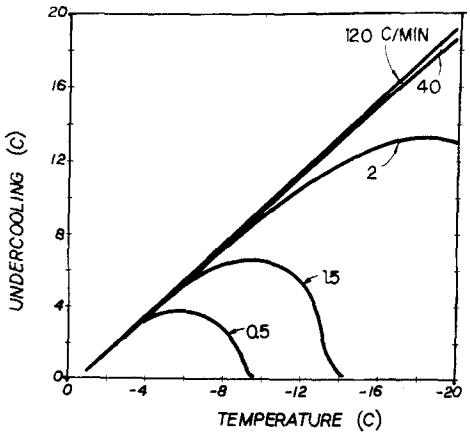

Fig. 6. Predicted undercooling of the cytoplasm of an oocyte suspended in isotonic saline. Extracellular seeding temperature is −0.615°C. Cooling rates are indicated on each curve

1.3°C/min was less than the observed volume fraction. Based on the results of this study, this discrepancy may be explained by the fact that they extrapolated the permeability from the suprazero temperature measurements.

The amount of the undercooling of the cytoplasm can be calculated using Fig. 5. Given the cell volume at an intermediate temperature the concentration of the intracellular solution can be estimated from the static behavior of oocytes depicted in Fig. 1. Then the osmolality of the intracellular solution can be converted to the equilibrium freezing temperature of the cytoplasm using the well-known $T_f = -1.858 \cdot$ osm relation. The cytoplasmic undercooling is the difference between the actual temperature and the equilibrium freezing temperature of the cytoplasm. The amount of intracellular undercooling as a function of temperature obtained from Fig. 5 is shown in Fig. 6 for different cooling rates. As can be seen from this figure, the amount of the intracellular undercooling becomes appreciable when the cooling rate exceeds 2°C/min. Qualitatively, this would mean high likelihood of intracellular ice formation at cooling rates greater than 2°C/min. The effect of water transport and the cytoplasmic undercooling on the intracellular ice formation is the subject of another paper (Toner, Cravalho & Karel, 1990*b*).

Distributed Behavior of Water Transport

Results of this study and others indicate that there is a great deal of individual variation in the permeability parameters in the same cell type (Cosman, 1983). In order to predict the osmotic behavior during freezing of mouse ova or any cell which has biophysical parameters widely distributed, it may not be sufficient to assume that a given cell will behave as the "mean" cell would as in Figs. 3, 5 and 6. The probability of a cell having a certain set of biophysical parameters needs to be coupled with that cell's osmotic behavior. A simple distributed parameter model of water transport is developed to address this issue. The basic approach used in this study is similar to the original model developed by Cosman (1983); however, a purely numerical solution is adopted in this study. Two major assumptions are made in the distributed parameter model: (i) the distribution of the biophysical parameters is due to actual variation in the parameters from ovum to ovum and not uncertainty in the experimental measurements, and (ii) the three distributed parameters used in this study, L_{pg}, E_{Lp} and SA/V, are assumed to be completely independent of each other. The numerical integration of Eq. (7) can be written symbolically

$$V = \text{function}(L_{pg}, E_{Lp}, SA/V, T). \tag{12}$$

The results of this study presented indicate that L_{pg}, E_{Lp} and SA/V are distributed parameters. The notation Λ_L, Λ_E and Λ_S denote the distribution or probability density function of permeability, activation energy and surface area-to-volume ratio, respectively. Using this notation, one finds at a specified cooling rate

$$\Lambda_V = \text{function}(\Lambda_L, \Lambda_E, \Lambda_S, T). \tag{13}$$

Equation (13) states that at each temperature a probability density function of volume Λ_V can be found by combining the probability density functions of the distributed parameters into the integration of Eq. (13). Practically, the volume probability density function can be determined by a computer model. In this model, the probability density functions of L_{pg}, E_{Lp}, SA/V are approximated by a finite number of representative values of these parameters. Associated with each value of the parameters is a probability. This probability can be most easily described as the likelihood that this value will occur relative to the other representative values. In the model, Eq. (13) is integrated using 4th-order Runge-Kutta scheme with a particular combination of representative values, and a volume/temperature curve is generated. The values of this curve are then rounded so that they can be sorted into a specified number of discrete volume levels. This integration of Eq. (13) is repeated with another combination of parameters, and another volume/temperature curve is generated. These integrations continue until every combination of the parameters has been used.

A weight is associated with each combination of parameters. This weight is simply the probability that that particular combination will occur, and it is equal to the product of the probabilities associated with each of the parameters in that combination. The probability density functions of each parameter were approximated by five points spaced one standard deviation apart starting two standard deviations less than the mean and continuing to two standard deviations more than the mean. This range corresponds to 98.7% of the cumulative distribution. Thus, there were 5^3 or 125 possible combinations of the three parameters. Figure 7 shows the volume probability density functions for various temperatures of the probability matrix for unfertilized mouse ova. As one can see, the probability density function is constrained to start at 100% probability when normalized volume is one at the extracellular nucleation temperature. As the cooling continues at 2°C/min, the function becomes more spread out because of the distributed values of the biophysical values. The function becomes skewed below −10°C since the volume is constrained at the equilibrium volume. Results agree qualitatively with the observed experimental volume curves depicted in Fig. 3. An important conclusion of this analysis is that any study of water transport at low cooling rates will have a large experimental discrepancy because of this distributed behavior of cells during freezing. This discrepancy can be estimated by using distributed permeability parameters in the solution of water transport model (Eq. (7)). However, at higher cooling rates, there will be no time for water transport and cells will remain approximately at their initial volume distribution during freezing.

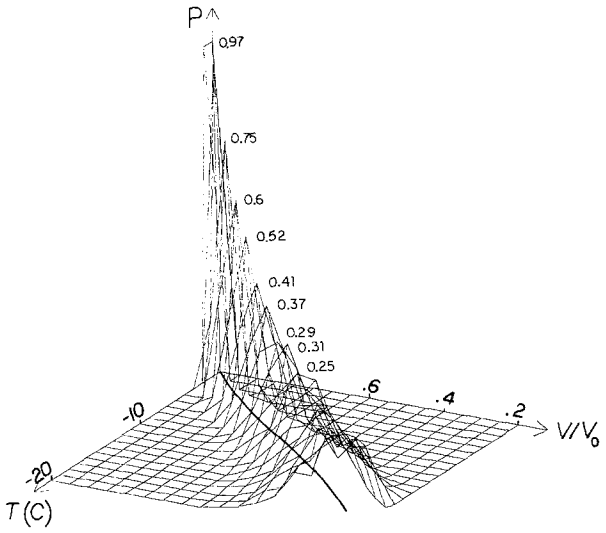

Fig. 7. Volume probability density functions as a function of temperature during freezing at 2°C/min in the absence of cryoprotectants. The solid line is the mean prediction

Estimation of Transmembrane Potential

The transmembrane potential during freezing can be modelled with Eq. (9) only if the water permeability of the plasma membrane is much higher than the ionic permeabilities (Silvares, 1974). The water permeability value determined in the previous section can be converted to the same units as ionic permeabilities as follows:

$$L_p = 0.8\ \mu\text{m/min-atm} = 14\ \text{cm}^3\text{/dyn-sec} \quad (14)$$

$$P_w = (L_p RT/v_w) = 20 \times 10^{-4}\ \text{cm/sec}. \quad (15)$$

This value is two orders of magnitude higher than the Cl^- permeability (10^{-6} cm/sec) and four orders of magnitude higher than Na^+ and K^+ permeabilities (10^{-8} cm/sec). Therefore one can assume that the osmotic equilibrium is reached before the ionic equilibrium. Internal ionic concentrations can then be estimated from the initial concentrations and the change in cell volume by neglecting the actual ionic diffusion across the membrane including the membrane potential independent Na-K-2Cl exchanger system (Geck & Heinz, 1986).

Once the internal ionic concentrations are estimated, the transmembrane potential can be evaluated from Eqs. (9) and (11). In addition, it is shown that Cl^- is passively distributed across the plasma membrane in mouse oocytes and Cl^- permeability is much higher than Na^+ and K^+ permeabilities (Powers & Tupper, 1975). Thus the Na^+ and K^+ dependent terms can be eliminated from Eq. (9). This is important because Eq. (9) becomes independent of ionic permeabilities and it only depends on the intra- and extracellular Cl^- concentrations. This means that the error introduced in our calculations by assuming constant ionic permeabilities is probably minimized. Figure 8 represents the computer simulation of the membrane potential in oocytes cooled at different rates. Equation (7) was solved using 4th-order Runge-Kutta method with a step size of 0.1°C. At the beginning of the freezing process (−1°C), the fast growth of ice in the extracellular solution causes a sharp increase of the membrane potential due to the instantaneous increase in extracellular ionic concentrations. As the temperature continues to drop, the oocyte dehydrates (*see* Figs. 3 and 5). The rate of increase of the internal Cl^- concentration will depend upon the dehydration (i.e., cooling rate), whereas the external Cl^- concentration is dictated by the equilibrium phase be-

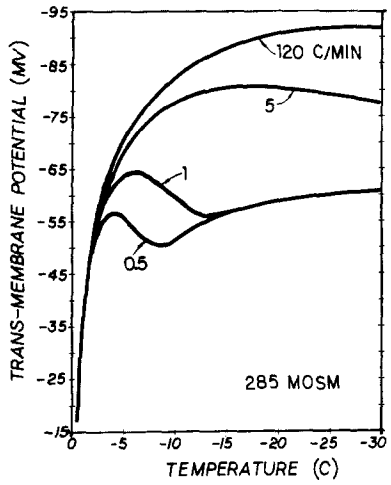

Fig. 8. Predicted temperature variation of the transmembrane potential in mouse oocytes. Cooling rates are indicated for each curve. Oocytes are suspended in isotonic saline solution. Extracellular ice is seeded at −1°C

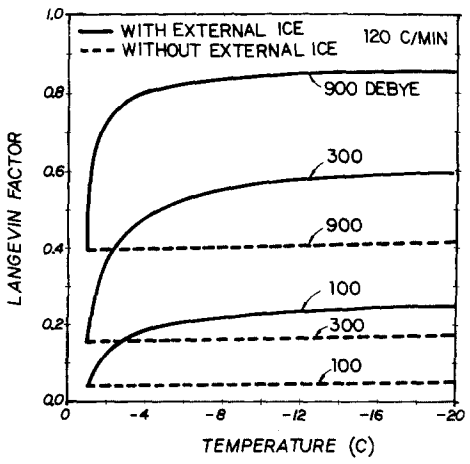

Fig. 9. Predicted dependence of dipole orientation (Langevin factor) on temperature during freezing at 120°C/min. Dipole moments are indicated for each curve. Dashed line represents the Langevin factor during cooling in the absence of extracellular ice

havior given by Eq. (11). There is a competition between the increase in intra- and extracellular Cl^- concentrations. Once the cell starts dehydrating as a function of the cooling rate, the rate of increase in internal Cl^- concentration may reach values higher than the rate of increase of the external Cl^- concentration, and the transmembrane potential may start decreasing in a certain range of temperature as shown in Fig. 8. At sufficiently low cooling rates, the minimum equilibrium cell volume may be reached; thereafter internal Cl^- will remain constant and E_m will increase due to the increase in external Cl^- concentration. This is clearly seen for cooling rate of 0.5°C/min in Fig. 8. As shown in Fig. 3 the oocyte reaches the minimum cell volume at −8°C, which corresponds to the increase in membrane potential displayed in Fig. 8. The change in membrane potential is substantial for almost all cooling regimes. Our estimations show that values as high as −90 mV can be reached during freezing. Unfortunately, there are no measurements of the transmembrane potential during freezing to quantify the predictions of this study.

Orientational Polarization

When an electrical field is applied across a membrane composed of proteins, lipids, and water each having a permanent dipole moment, the dipoles will be subjected to a torque. This torque will try to align the dipoles with the electrical field in the presence of thermal agitations opposing the orientation (Pethig, 1979; Zimmermann, 1982). The Langevin factor gives the percentage of dipoles for a given dipole moment that are aligned due to the applied electrical field (Pethig, 1979)

$$L(\Lambda) = \coth \Lambda - (1/\Lambda) \tag{16}$$

where $L(\Lambda)$ is called the Langevin factor, $\Lambda = \mu_d E_m / kT$, k is the Boltzmann constant, and μ_d is the dipole moment (Pethig, 1979). Equation (16) can be coupled with Eqs. (7) and (9) to predict the dipole orientation during freezing. Figure 9 shows the solution of Eq. (16) for a freezing protocol in isotonic saline at 120°C/min. The Langevin function $L(\Lambda)$ is plotted as a function of temperature during freezing for different dipole moments. As can be seen from this figure, molecules with larger dipole moments will align at higher proportions with the electrical field. The dipole moment for most of the proteins is on the order of 300 debye and greater (Pethig, 1979; Zimmerman, 1982). For proteins with 300 debye dipole moment, the percentage of dipoles aligned with the membrane potential increases from 16% at 0°C prior to freezing to 58% at −8°C after the seeding of the external ice, and subsequent cooling. Also shown in Fig. 9, cooling in the absence of external ice does not result in substantial orientational polarization since external ionic strength remains constant. Water molecules have a dipole of 1.8 debye. Therefore, the orientation of water molecules in the membrane will be very small and can be easily ignored. The change in the polarization of the plasma membrane proteins and lipids during freezing may affect the kinetics of intracellular ice formation as

well as the water transport across the membrane. It should be emphasized here that these calculations are based on a very simple model of membrane, as such the conclusions of this study should be considered only speculative until experimental verification becomes available.

In summary, analysis of the water transport across the plasma membrane of mouse oocytes during freezing showed that there are substantial changes in volume and undercooling of the internal milieu, depending on the cooling rate. Although, there is no significant discontinuity in the permeability between +30 and −20°C, it is still not acceptable to extrapolate the permeability parameters from suprazero temperature range to predict the freezing behavior of mouse oocytes. In addition to water transport, a simple model of the transmembrane potential suggests that the formation of external ice may result in substantial orientational polarization of the membrane proteins and lipids. Both water transport and transmembrane potential during freezing are important parameters in describing the physicochemical events occurring during freezing of biological cells. Their accurate knowledge is necessary to better understand the mechanisms of freeze/thaw injury and intracellular ice formation.

The authors would like to express their gratitute to Dr. M.D. Cosman and J. Kandel of Interface Techniques Company, Cambridge, and Dr. A. Hubel and M. Orrico of Massachusetts Institute of Technology for their support and help. We are indebted to Dr. J.D. Biggers, Dr. A.A. Kiessling, and K.V. Jackson of Harvard Medical School for helpful discussions. Funding for this study was provided in part by a grant (to D.R.A.) from the Milton Fund, Harvard University. Also we wish to thank NIDDK and the National Pituitary Program for providing PMSG for these studies.

Nomenclature

a	Activity	
A	Surface area of cell	[μm^2]
B	Cooling rate	[°C/min]
D	Diameter	[μm]
E_{Lp}	Activation energy	[kcal/mol]
E_m	Membrane potential	[mV]
F	Faraday constant	[9.6487 10^7 C/kg-mol]
ΔH_f	Heat of fusion	[kcal/mol]
$[j]$	Concentration of j'th ion	[mM]
k	Boltzmann constant	[1.3806 10^{-23} J/K]
L_p	Permeability of membrane	[$\mu m^3/\mu m^2$-min-atm]
L_{pg}	Reference water permeability	[$\mu m^3/\mu m^2$-min-atm]
N	Number of moles	[mol]
P_j	Ionic permeability of j'th ion	[cm/sec]
PA	Projected area	[μm^2]
R	Gas constant	[.001986 kcal/mol-K]
SA/V	Surface area-to-volume ratio	[μm^{-1}]
T	Temperature	[K or C]
t	Time	[sec]
V	Volume	[μm^3]
v	Partial molar volume	[μm^3/mol]
x	Mole fraction	
v_s	Dissociation coefficient	
Λ	Langevin factor	
μ_d	Dipole moment	[debye]
π	Osmolality	[osm/kg H_2O]
χ	Chi-square	

Superscripts

ex	extracellular
in	intracellular

Subscripts

b	osmotically inactive
R	reference
o	initial
s	solute
w	water

References

Abramczuk, J., Sawicki, W. 1974. Variation in dry mass and volume of nonfertilized oocytes and blastomeres of 1-, 2- and 4-celled mouse embryos. *J. Exp. Zool.* **188:**25–34

Bernard, A., McGrath, J.J., Fuller, B.J., Imoedemhe, D., Shaw, R.W. 1988. Osmotic response of oocytes using a microscope diffusion chamber: A preliminary study comparing murine and human ova. *Cryobiology* **25:**495–501

Biggers, J.D., Borland, R.M., Powers, R.D. 1977. Transport mechanisms in the preimplantation mammalian embryo. *In:* The Freezing of Mammalian Embryos. K. Elliott and J. Whelan, editors. pp. 129–153. Ciba Foundation Symposium, Elsevier, New York

Callow, R.A., McGrath, J.J. 1985. Thermodynamic modelling and cryomicroscopy of cell-size, unilamellar, and paucilamellar liposomes. *Cryobiology* **22:**251–267

Cosman, M.D. 1983. Effect of Cooling Rate and Supercooling on the Formation of Ice in a Cell Population. Ph.D. Thesis. Massachusetts Institute of Technology, Cambridge

Cosman, M.D., Toner, M., Kandel, J., Cravalho, E.G. 1989. An integrated cryomicroscopy system. *Cryo-Letters* **10:**17–38

Diller, K.R., Cravalho, E.G. 1970. A cryomicroscope for the study of freezing and thawing processes in biological cells. *Cryobiology* **7:**191–199

Frumento, A.S. 1965. The electrical effects of an ionic pump. *J. Theor. Biol.* **9:**253–262

Geck, P., Heinz, E. 1986. The Na-K-Cl contransport system. *J. Membrane Biol.* **91:**97–105

Geduldig, D. 1968. Analysis of membrane permeability coefficient ratios and internal ion concentrations from a constant field equation. *J. Theor. Biol.* **19:**67–78

Goldman, D.E. 1943. Potential, impedance, and rectification in membranes. *J. Gen. Physiol* **27:**37–60

Hendl, A., McGrath, J.J., Olien, C.R. 1987. On the adhesive interaction between ice and the mouse oocyte. *Cryo-Letters* **8:**334–345

Hodgkin, A.L., Katz, B. 1949. The effect of sodium ions on the electrical activity of the giant axon of the squid. *J. Physiol (London)* **108:**37–77

Jackowski, S., Leibo, S.P., Mazur P. 1980. Glycerol permeabilities of fertilized and unfertilized mouse ova. *J. Exp. Zoology* **212:**329–341

Jackson, K.V., Kiessling, A.A. 1989. Fertilization and cleavage of mouse oocytes exposed to the conditions of human oocyte retrieval for in vitro fertilization. *Fertil. Steril.* **51:**675–681

Kotyk, A., Janacek, K., Koryta, J. 1988. Biophysical Chemistry of Membrane Functions. John Wiley & Sons, New York

Leibo, S.P. 1980. Water permeability and its activation energy of fertilized and unfertilized mouse ova. *J. Membrane Biol.* **53:**179–188

Leibo, S.P., McGrath, J.J., Cravalho, E.G. 1978. Microscopic observations of intracellular ice formation in unfertilized mouse ova as a function of cooling rate. *Cryobiology* **15:**257–271

Levin, R.L., Cravalho, E.G., Huggins, C.E. 1976. A membrane model describing the effect of temperature on the water conductivity of erythrocyte membranes at subzero temperatures. *Cryobiology* **13:**419–429

Levin, R.L., Ushiyama, M., Cravalho, E.G. 1979. Water permeability of yeast cells at sub-zero temperatures. *J. Membrane Biol.* **46:**91–124

Mansoori, G.A. 1975. Kinetics of water loss from cells at subzero centigrade temperatures. *Cryobiology* **12:**34–45

Mazur, P. 1963. Kinetics of water loss from cells at subzero temperatures and likelihood of intracellular freezing. *J. Gen. Physiol.* **47:**347–369

Mazur, P. 1984. Freezing of living cells: Mechanisms and implications. Am. J. Physiol. **143:**C125–C142

Mazur, P., Schneider, U. 1986. Osmotic response of preimplantation mouse and bovine embryos and their cryobiological implications. *Cell Biophys.* **8:**259–285

Modell, M., Reid, R.C. 1983. Thermodynamics and Its Applications. Prentice-Hall, Englewood Cliffs, NJ

Ohki, S. 1986. Membrane potential of squid axon. *In:* Electrical Double Layers in Biology. M. Blank, editor. pp. 103–118. Plenum, New York

Orrico, M. 1988. Water Permeability of Mouse Ova and Predicted Osmotic Behavior During Freezing. M.S. Thesis. Massachusetts Institute of Technology, Cambridge

Pethig, R. 1979. Dielectric and Electronic Properties of Biological Materials. John Wiley & Sons, New York

Pethig, R. 1986. Ion, electron, and proton transport in membranes: A review of the physical processes involved. *In:* Modern Bioelectrochemistry. F. Gutmann and H. Keyzer, editors. pp. 199–239. Plenum, New York

Powers, R.D., Tupper, J.T. 1975. Ion transport and permeability in the mouse egg. *Expt. Cell. Res.* **91:**413–421

Rall, W.F., Mazur, P., McGrath, J.J. 1983. Depression of the ice-nucleation temperature of rapidly cooled mouse embryos by glycerol and dimethyl sulfoxide. *Biophys. J.* **41:**1–12.

Scheiwe, M.W., Koerber, C. 1983. Basic investigations on the freezing of human lymphocytes. *Cryobiology* **20:**257–273

Schwartz, G.J., Diller, K.R. 1983*a*. Osmotic response of individual cells during freezing: II. Membrane permeability analysis. *Cryobiology* **20:**542–552

Schwartz, G.J., Diller, K.R. 1983*b*. Analysis of the water permeability of human granulocytes at subzero temperatures in the presence of extracellular ice. *Trans. ASME* **105:**360–365

Shabana, M., McGrath, J.J. 1988. Cryomicroscopic investigation and thermodynamic modelling of the freezing of unfertilized hamster ova. *Cryobiology* **25:**338–354

Silvares, O.M. 1974. A thermodynamic model of water and ion transport across the membrane during freezing and thawing: the human erythrocyte. Ph.D. Thesis. Massachusetts Institute of Technology, Cambridge

Silvares, O.M., Cravalho, E.G., Toscano, W.M., Huggins, C.E. 1975. The thermodynamics of water transport from biological cells during freezing. *Trans. ASME J. Heat Transfer* **97:**582–588

Stusnick, E., Hurst, R.P. 1972. Numerical determination of membrane permeability analysis. *J. Theor. Biol.* **37:**261–271

Tondorf, S., McGrath, J.J., Olien, C.R. 1987. On the adhesive interaction between ice and cell-size liposomes. *Cryo-Letters* **8:**322–333

Toner, M., Cravalho, E.G., Armant, D.R. 1990*a*. Cryomicroscopic analysis of intracellular ice formation in mouse oocytes without cryoadditives. *Cryobiology (in press)*

Toner, M., Cravalho, E.G., Karel, M. 1990*b*. Thermodynamics and kinetics of intracellular ice formation during freezing of biological cells. *J. Applied Phys.* **67:**1582–1593

Weast, R.C. 1973. Handbook of Chemistry and Physics. (54th ed.) CRC, Cleveland (OH)

Zimmermann, U. 1982. Electric field-mediated fusion and related electrical phenomena. *Biochim. Biophys. Acta* **694:**227–277

Received 31 August 1989; revised 20 November 1989